Prediction of Hydrodynamic and Structural Behavior of V- Fin Depressors

Jithin P.N., Afsy Makkar, Rakhi Ajayakumar, Kiran Jacob

Abstract— Oceanographic applications require an underwater body to be moved deep under the water column. This is usually facilitated by towed cable array system. A hydrodynamic depressor is a well-known tool used in oceanographic practice for the purpose of generating depressive force (downward force) and supporting towed systems at fixed depth. The present study focus on CFD analysis in ANSYS FLUENT on V- Fin depressors with two types of wing configuration (NACA 0012 and NACA 0015). The hydrodynamic characteristics such as lift and drag forces, lift and drag coefficients, velocity and pressure distribution around the depressor are evaluated at a speed of 5 and 10 knots by varying the angle of attack (AOA). The structural analysis of the depressor configuration is carried out in ANSYS workbench. It was found that V-fin depressor with NACA 0015 wing configuration provided maximum negative lift and structural strength when compared with NACA 0012 at different towing speeds and AOA.

Index Terms— Angle of attack (AOA), NACA, deformation, domain, drag force, lift force, towing speed, V- Fin depressor, wing span, airfoil

1 Introduction

MANY marine applications such as sea bed mapping, mine detection, naval applications, towing of sonar arrays require an underwater body or vehile to be towed by the vessel at a pre- determined depth without get affected by surrounding noises. This is usually facilitated by towed cable array system. The possible towing systems available are single part towing system and two part towing system. Single part underwater towing system is consisting of a towing cable connecting the towed body with the towing vessel. The towed body becomes shallow as the towing vessel speed increases which can only be adjusted by increasing the tow cable length. This result in increased cable tension, drag force and hence requires a massive array handling system. The two part underwater towed system (Fig.1) maintains an underwater towed vehicle to move stable while operating under different towing speeds.

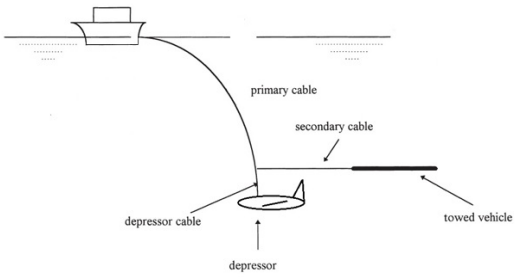

Fig. 1. Two part towing system with depressor

- *Jithin P.N. is currently working as Asst. Professor in Dept. of Mechanical Engineering, Rajagiri School of Engineering & Technology, Kochi, Kerala, India. E-mail: jithinpn@rajagiritech.edu.in*
- *Afsy Makkar is currently pursuing masters degree program in Computer Aided Structural Engineering from ICET, Muvattupuzha, Ernakulam affliated to KTU, Tvpm, Kerala, India. E-mail: afsymakkar@gmail.com*
- *Rakhi Ajayakumar is currently working as Asst. Professor in Dept. of Civil Engineering, CISAT, Ernakulam, Kerala, India.*
- *Kiran Jacob is currently working as Asst. Professor in Dept. of Civil Engineering, ICET, Muvattupuzha, Ernakulam, Kerala, India.*

Depressor is a device that gives a depressive force on the under water towed body and helps it to be towed at a particular depth. Hydrodynamic depressors are those which provide the depressive force derived from the negative lift created by the depressor wings. It decouples the towed body from the induced ship motions and ensures the stability.

The principles and design of the underwater towed bodies and depressors have been developed and investigated by many researchers by different methods. Wilburn L. Moore [13] has studied on bodies of revolution with high cavitation -inception speeds - for application to the design of hydrofoil-boat nacelles. D. C. Summey [1] conducted a study on hydrodynamic design and analysis of a towed environmental sensor vehicle for the Naval Coastal Systems Center (NCSC). P. Rispin and J.S. Diggs [9] researched on at-sea trial evaluation of the hydrodynamic performance and stability of a simulated depressor-towed array system for the Office of Naval Research (ONR). R. F. Becker [10] conducted study on high speed sonar array depressor. It's directed towards the development of a high-speed, lightweight depressor for towing a sonar array from surface ships. Roger E. Race [11] presented a paper on the variable depth V-Fin Depressor. He used ENDECO Type 1074 variable depth V-Fin depressor which provides a remote controlled towed vehicle that can carry a multitude of sensors. Jiaming Wu and Allen T. Chwang [4] studied on a hydrodynamic model of a two-part underwater towed system. Jiaming Wu and Allen T. Chwang [5] conducted an experimental investigation on a two-part underwater towed system in a ship towing tank. The hydrodynamic performance of a two-part underwater towed system in waves is examined experimentally. Steven D. Miller [12] studied on lift, drag and moment of a NACA 0015 airfoil in a low speed wind tunnel at varying angles of attack. Husainie S.N and Qamar .A [3] conducted a wind tunnel and airfoil drag analysis on NACA 0015 airfoil section. Jithin P. N and Senthil Prakash M. N [8] conducted a numerical investigation on the hydrodynamic behavior of the depressor. He carried out CFD analysis of a hydrodynamic depressor using the software FLUENT.

International Journal of Scientific & Engineering Research, Volume 8, Issue 5, May-2017
ISSN 2229-5518

2 V- FIN DEPRESSOR

V-Fin depressor is a stable, lightweight platform used to deploy instruments from a moving vessel. It is designed to dive deep in the water column to collect data, minimizing the amount of cable required. Proper hydrodynamic design is necessary in order to achieve the effective performance of a depressor. A non-hydrodynamic shape can cause excessive drag, noise and instability even at low speeds. Since the depressor is an underwater body, it's important to study about various hydrodynamic forces acting on it.

2.1 Model Specification

In this study a V-Fin depressor with two types of main wing cross section (NACA 0012 and NACA 0015) are modelled using CATIA V5.

The standard specifications [14] of V-Fin depressor is given below:

Length, L : 2 feet = 609.6mm

Wingspan, W : 28.5 inch = 723.9mm

Height, H : 13.75 inch = 349.25mm

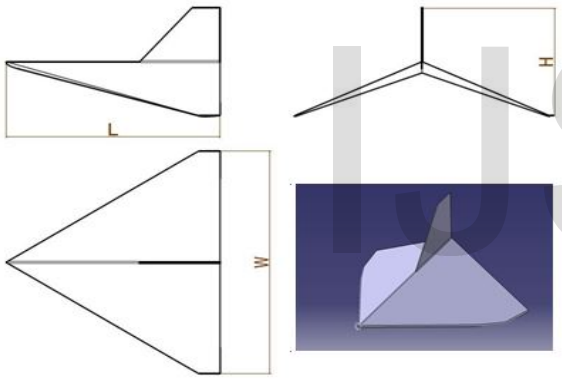

Fig. 2. Depressor model

3 CFD ANALYSIS

The governing equation of any CFD problem is the Navier - Stoke's equation. The general conservative form of the Navier - Stoke's equation is given below.
Continuity equation,

$$\frac{\partial \rho}{\partial t}+\frac{\partial}{\partial x_i}(\rho u_i)=0 \qquad (1)$$

Where, ρ = density, u_i is the velocity component in the i^{th} direction i =1, 2, 3.

The density is constant in case of incompressible flows and so the continuity equation gets modified as,

$$\frac{\partial}{\partial x_i}(\rho u_i)=0 \qquad (2)$$

Momentum or Navier - Stoke's equation,

$$\frac{\partial}{\partial t}(\rho u_i)+\frac{\partial}{\partial x_j}(\rho u_i u_j)=-\frac{\partial p}{\partial x_i}+\frac{\partial \tau_{ij}}{\partial x_j}+\rho g_i \qquad (4)$$

$$\tau_{ij}=[\mu(\frac{\partial u_i}{\partial x_j}+\frac{\partial u_j}{\partial x_i})]-\frac{2}{3}\mu\frac{\partial u_l}{\partial x_l}\delta_{ij} \qquad (5)$$

Where,

τ_{ij} = Reynolds stress tensor, p = static pressure, g_i = gravitational acceleration in the ith direction, δ_{ij} is the Kroneker delta and is equal to unity when i= j; and zero when i ≠ j.

The Reynolds-Averaged form of the above momentum equation including the turbulent shear stresses is given by

$$\frac{\partial}{\partial t}(\rho U_i)+\frac{\partial}{\partial x_j}(\rho U_i U_j)=\frac{\partial}{\partial x_j}\left[\mu\left(\frac{\partial u_i}{\partial x_j}+\frac{\partial u_j}{\partial x_i}\right)-\left(\frac{2}{3}\mu\frac{\partial u_l}{\partial xl}\right)\right] -\frac{\partial p}{\partial x_i}+\frac{\partial}{\partial x_j}\left(-\rho\overline{u_i' u_j'}\right) \qquad (6)$$

Where,

u_i' is the instantaneous velocity component at i = 1, 2, 3.

$\left(-\rho\overline{u_i' u_j'}\right)=Rij$

R_{ij}, is called the Reynolds stress.

For the closure of the RANS equation a turbulence model is used (Standard k-ε turbulence model). The standard k-ε turbulence model is the most widely employed two- equation eddy-viscosity model. It is based on the solution of equations for the turbulent kinetic energy and the turbulent dissipation rate.

3.1 Validation of CFD Analysis

For validation of the CFD simulation it is necessary to compare the results with available experimental results. Validation is important as it will help one to know about the percentage of error that may happen for our present analysis of V- Fin depressor. Experimental results of wind tunnel test of NACA 0015 airfoil section of chord length 8 inch and 100 mm thickness are available in the report of Steven D. Miller [12]. A similar airfoil model is constructed using CATIA V5 and a CFD analysis is performed at a nominal wind velocity of 17 m/s using ANSYS FLUENT. Computational domain for the analysis have length equal to chord length of the airfoil towards upstream and four times the chord length towards downstream. The domain has a height equal to chord length towards both up and downward direction. The domain specifi-

International Journal of Scientific & Engineering Research, Volume 8, Issue 5, May-2017
ISSN 2229-5518

cation for the airfoil analysis is shown in Fig. 3. Boundary condition for the analysis is highlighted in Table 1. Tetrahedral meshes with inflation layers are provided around the airfoil surface for capturing the pressure and velocity variations near to the surface.

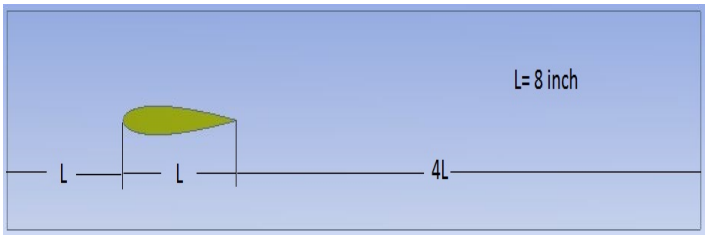

Fig. 3. Domain specification for airfoil

TABLE 1
BOUNDARY CONDITIONS

Domain Surface	Boundary Condition
Inlet	Velocity inlet (17 m/s)
outlet	Pressure outlet (1 bar)
Domain wall and airfoil surface	Wall with no slip condition

The 3D Reynolds Averaged Navier- Stokes equations (RANS) are solved in combination with the Standard k-ε turbulence model using ANSYS FLUENT. Semi- Implicit method (SIMPLE) is chosen for pressure velocity coupling in order to induce a constraint on the solution. Pressure interpolation is standard and first order discretization schemes are used for both convection and viscous terms of the governing equation.

3.2 Comparison of CFD and experiment results

The coeffient of lift (C_L) values obtained from CFD simulations have compared with the experimental C_L values available in the report of Steven D. Miller [12] and was found to have close agreement. The analysis were carried out for three different positive angle of attack (AOA) of the airfoil. At higher angle of attack the results come much closer to the experimental values. The results are highlighted in Table 2. The pressure contour on top and bottom surface of the airfoil is shown in Fig. 4.

TABLE 2
COMPARISON OF CFD AND EXPERIMENTAL RESULTS

ANGLE OF ATTACK	EXPERIMENTAL	ANSYS FLUENT
	C_L	C_L
0^0	-0.0044	-0.007
5^0	0.5438	0.42
10^0	0.9067	0.92

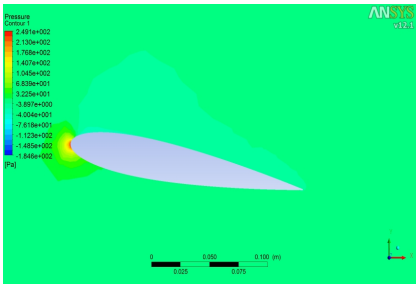

Fig. 4. Pressure contour of airfoil at 15^0 AOA

3.3 Computational domain and mesh details for depressor analysis

The V- Fin depressor is enclosed inside a rectangular box type fluid domain. The fluid domain extends to a distance equal to the length of the depressor body along upstream direction and 4 times along downstream to achieve reliable application of boundary conditions. The height of the domain is two times the height of the depressor in both upward and downward direction from extreme depressor surface points. The width of the domain is 2 times the wingspan from the wing ends. The details of the domain length and height are shown in the Fig. 5.

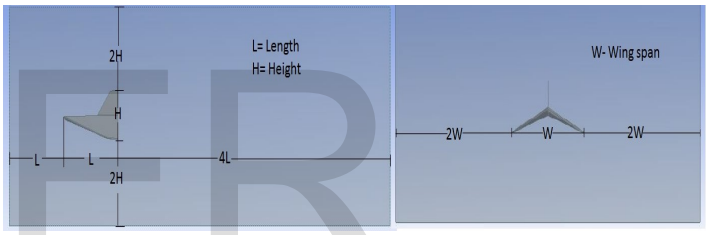

Fig. 5. Depressor domain specification

During the preprocessing the meshing of the depressor with unstructured tetrahedral mesh is carried out. The descretized domain is shown in Fig. 6. Unstructured meshing allows meshing of complex geometry with in lesser time. Unstructured meshes are used in many FEA and CFD applications, which have irregular shape of object or region of interest.

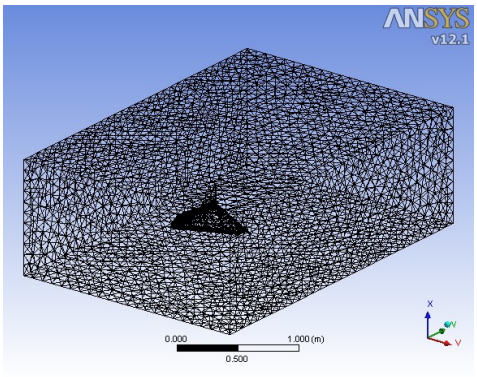

Fig. 6. Meshed fluid domain

Unlike structured mesh, they can have arbitrary topology in a confined region. In unstructured meshes points are laid in the region of interest in a random order forming triangular sub division of the region. For the preset study unstructured

International Journal of Scientific & Engineering Research, Volume 8, Issue 5, May-2017
ISSN 2229-5518

tetrahedral meshes with inflation layers near to the depressor body surface is provided. The inflation layers are triangular prism mesh arranged in layers which are capable of capturing flow conditions near to the surface of the depressor.

3.4 Boundary Conditions

The fluid domain is a rectangular volume with depressor suppressed. The flow is assumed to be steady and three-dimensional. The depressor is assumed to be operated at a depth of 15m from sea level and so the gauge pressure at the oulet face is set to 150828.75 Pa. The boundary conditions given to different zones are as highlighted in Table 3.

TABLE 3
BOUNDARY CONDITION FOR DEPRESSOR DOMAIN

Zone	Boundary Condition
Inlet Face	Velocity inlet (at 5 and 10 Knots)
Outlet face	Pressure outlet (Gauge pressure set to 150828.75 Pa)
Domain wall	Wall with specified shear condition
Depressor surface	Wall with no slip condition

The 3D Reynolds Averaged Navier- Stokes equations (RANS) are solved with standard k-ε turbulence model as the Reynolds number is above 10^6 and the flow is external. It is the simplest or most complex models of turbulence among two-equation models in which the solution of two separate transport equations allow the turbulent velocity and length scales to be independently determined. Semi- Implicit method (SIMPLE) is chosen for pressure velocity coupling in order to induce a constraint on the solution. Pressure interpolation is standard and second order discretization schemes are used for both convection and viscous terms of the governing equation.

3.5 Results and discussion of CFD results

The CFD analysis is carried out with V- Fin depressor (NACA 0015 and 0012 wing configuration) moving at a towing speed of 5 and 10 knots at different negative angle of attack of 0^0, 5^0, 10^0 and 15^0. The negative lift force and drag force generated at these negative angle of attack was calculated and the the results are highlighted in the Fig. 7. It was observed that the downward force generated at both towing speeds by V-fin depressor with NACA 0015 wing configuration is higher when compared with the NACA 0012 wing configuration. Similar is the case for the drag force generated. The pressure variations at the bottom and top surface of the main wings of the depressor for both type of depressors are shown in the Fig. 8. At 10 knots the V-fin depressor with NACA 0015 wing configuration is generating lift force of about 2799 N. The pattern of the simulation results are as per the wing theory that the lift force and drag force increases as the angle of attack of the wing of the depressor increases. It also increases as the towing speed of the depressor increases. As shown in Fig. 8. When fluid flow around the depressor body a high pressure region is created on the top surface of the depressor wings compared to the bottom surface which inturn creates a net downward force on the depressor body. This pressure difference increases at higher angle of attack and high towing speeds and so the depressive force increases. It can be observed from Fig. 8 that for depressor with NACA 0015 wing configuration a low pressure of the range 1.504 e^{05} Pa to 1.498 e^{05} Pa is generated at the bottom surface of the wings. On the top surface of the wings a pressure range of 1.5165 e^{05} Pa to 1.510 e^{05} Pa is generated. The net average downward pressure on the body of the depressor (NACA 0015 wing configuration) is about 1.225 e^{-02} Pa. For depressor with NACA 0012 wing configuration bottom surfsce of the wing is acted by a low pressure ranging between 1.501 e^{05} Pa to 1.506 e^{05} Pa. The top surafce of the wings is acted by a pressure ranging between 1.511 e^{05} Pa to 1.5155 e^{05} Pa. The net average downward pressure on the body of the depressor (NACA 0012 wing configuration) is about 0.975 e^{-02} Pa. Thus V-fin depressor with NACA 0015 wing configuration is generating higher downward force in all the cases considered for simulation.

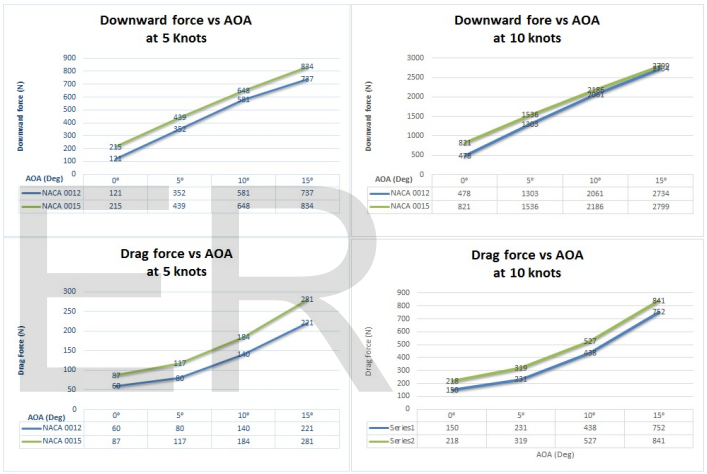

Fig. 7. Negative lift and drag forces generated at different AOA

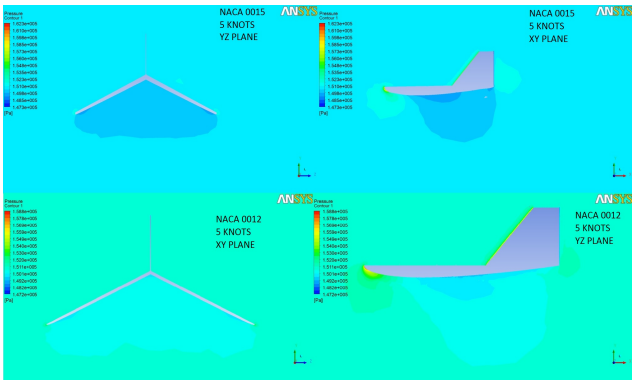

Fig. 8. Comparison of pressure contour at 0^0 AOA

4 STRUCTURAL ANALYSIS

The structural analysis of the V- Fin depressor was carried out in ANSYS Structural workbench. The depressor material is selected as steel with properties applied. Material is assumed to be isotropic with poisson's ratio 0.3. The depressor body is assumed to be a beam element fixed at its nose end which re-

International Journal of Scientific & Engineering Research, Volume 8, Issue 5, May-2017
ISSN 2229-5518

sembles a cantilever beam. The pressure generated due to the fluid flow around the depressor body is imported from FLUENT solver as the load condition for the structural analysis. The structural analysis is performed for both the wing configuration for all the angle of attack at two towing speeds same as in which the CFD analysis is performed. A comparison of the deformation of the depressor body fixed at its nose end for both NACA 0015 and 0012 wing configuration is carried out. It can be observed from the Fig. 9 that the maximum deformation of the body happens at the tail region of the depressor in both the cases and depressor with wing configuration 0012 deforms more. Fig. 10 represents graph which gives a comparison of maximum deformation over the body of both configuration of the depressor at different towing speed and AOA.

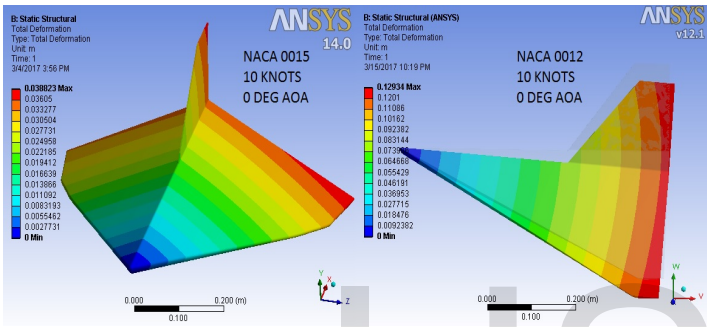

Fig. 9. Comparison of deformation at 10 knots speed and 0^0 AOA

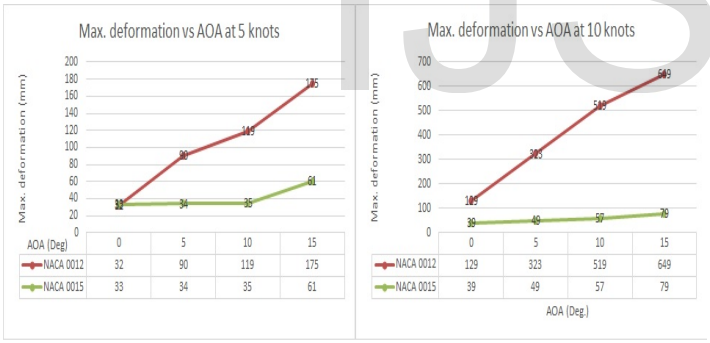

Fig.10. Comparison of deformation at 5 and 10 knots towing speed

It can be observed from Fig. 10 that V- Fin depressor with wing configuration NACA 0012 deforms more than NACA 0015 configuration. Depressor with wing configuration NACA 0012 deforms to a maximum value of 175 mm at 5 knots and 15 degree AOA and to 695 mm at 10 knots and 15 degree AOA. Since the depressor is fixed to the nose end, the von mises stress is concentrated more on the nose tip as shown in the Fig. 11. Similar is the case for both configurations at all towing speeds and AOA. It can be observed from Fig. 11 which shows the Von- mises stress distribution over the body of the V- Fin depressor with NACA 0015 wing configuration at 10 knots towing speed and 0^0 AOA. A stress ranging from 8849.3 Pa to 5.91 e^8 Pa is acting on the depressor body. At the nose tip it reaches to 8.27 e^8 Pa.

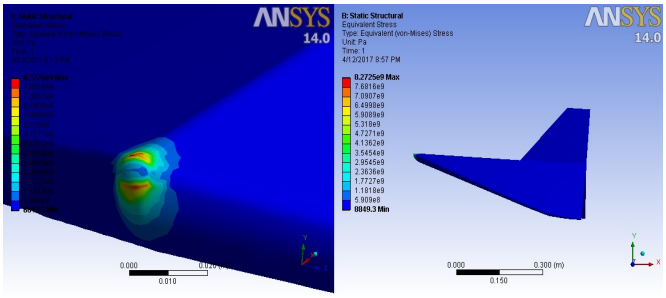

Fig. 11. Stress distribution over V- Fin depressor with NACA 0015 wing configuration at 0^0 AOA and 10 knots towing speed

The Table 4 below shows the average stress over the body of the V- Fin depressor at different towing speeds and AOA.

TABLE 4
AVERAGE VON- MISSES STRESS OVER V-FIN DEPRESSOR BODY

Towing Speed	AOA (Deg.)	Von- mises stress NACA 0015 (Pa)	Von- mises stress NACA 0012 (Pa)
5 knots	0	3.69 e^8	2.65 e^8
	5	2.72 e^8	7.23 e^8
	10	2.69 e^8	11.23 e^8
	15	3.5 e^8	15.8 e^8
10 knots	0	2.95 e^8	11.1 e^8
	5	4.02 e^8	28.13 e^8
	10	4.53 e^8	43.8 e^8
	15	5.26 e^8	53.3 e^8

The average von- mises stress generated over the body of the V- Fin depressor is more for wing configuration NACA 0012 in all the cases and so it is more prone to deformation and can leads to damage easily.

5 CONCLUSION

V- Fin depressor with two types of wing configuration NACA 0012 and NACA 0015 are modelled in CATIA V6. CFD analysis were conducted at 5 and 10 knots towing speed and various AOA (0^0, 5^0, 10^0 and 15^0). Structural analysis were also conducted to find the stress distribution and deformation of the depressor at similar towing conditions and AOA. The V- Fin depressor with NACA 0015 wing configuration outperformed NACA 0012. The negative lift generated by NACA 0015 is greater than NACA 0012 in all towing speeds and AOA. Moreover the deformation of NACA 0012 is more than NACA 0015 in all towing speed and angle of attack.

It is also important to mention the limitations of this analysis. Firstly for CFD analysis the effect of wave and current forces is not considered. The fluttering effect of the cable on towed body is not considered. For structural analysis the nose tip of the depressor is assumed to be fixed such that the cable is considered to be rigid and inextensible.

International Journal of Scientific & Engineering Research, Volume 8, Issue 5, May-2017
ISSN 2229-5518

5 REFERENCES

[1] D. C. Summey [1980], "Hydrodynamic design and analysis of a towed environmental sensor vehicle", NCSC, pp: 1-48.

[2] David Hopkin, Jon M.Preston, Sonia Latchman [1993], "Effectiveness of a Two-Part Tow for Decoupling Ship Motions" Defence Research Establishment Pacific, IEE, pp: 359-364.

[3] Husainie S. N., Qamar A. [2010], "Wind Tunnel and airfoil drag analysis", International journal on Ocean Engineering. pp: 220–232.

[4] [Jiaming Wu, Allen T. Chwang [2000], "A hydrodynamic model of a two-part underwater towed system", International journal on Ocean Engineering .No.27 pp: 455–472.

[5] Jiaming Wu, Allen T. Chwang [2001], "Experimental investigation on a two-part underwater towed system", International journal on Ocean Engineering, No. 28, pp: 735–750.

[6] Jiaming Wu, Allen T. Chwang [2001], "Investigation on a two-part underwater manoeuvrable towed system", International journal on Ocean Engineering .No.28 pp: 1079–1096.

[7] Jiaming Wu et al. [2005], "Experimental study on a controllable underwater towed system", International journal on Ocean Engineering, No. 32, pp: 1803–1817.

[8] Jithin P.N., Senthil Prakash M. N. [2014], "Hydrodynamic behavior of the depressor", International journal of mechanical engineering and robotics research, Vol. 3, No. 1, pp: 256-264.

[9] P. Ripsin, J. S. Diggs [1981], "'At-sea trial evaluation of the hydrodynamic performance and stability of a simulated depressor-towed array system", Office of Naval Research, DTNSRDC, Maryland.

[10] R. F. Becker [1981], "High speed sonar array depressor", Program final report, Prepared for Office of Naval Research, Virginia.

[11] Roger E. Race [1985], "The variable depth V-Fin Depressor", Oceans 85-Ocean engineering and the environment, pp: 1013-1018.

[12] Steven D. Miller [2008], "Lift, drag and moment of a NACA 0015 airfoil", International journal on Ocean Engineering, pp: 180-210.

[13] Wilburn L. Moore [1962], "Bodies of revolution with high cavitation-inception speeds - for application to the design of hydrofoil-boat naceiles", Department of navy, DTMB, pp: 1-28.